CHALMERS
UNIVERSITY OF TECHNOLOGY

Computationally efficient algorithm for optimal battery preconditioning and charging of electric vehicles

Downloaded from: https://research.chalmers.se, 2025-05-23 18:58 UTC

Citation for the original published paper (version of record):
Montalto, L., Murgovski, N., Fredriksson, J. (2024). Computationally efficient algorithm for optimal battery preconditioning and charging of
electric vehicles. IEEE Conference on Intelligent Transportation Systems, Proceedings, ITSC, 2024: 1600-1605. http://dx.doi.org/10.1109/ITSC58415.2024.10920033

N.B. When citing this work, cite the original published paper.

© 2024 IEEE. Personal use of this material is permitted. Permission from IEEE must be obtained for all other uses, in any current or future media, including reprinting/republishing this material for advertising or promotional purposes, or reuse of any copyrighted component of this work in other works.

(article starts on next page)

Computationally efficient algorithm for optimal battery preconditioning and charging of electric vehicles

Lorenzo Montalto, Nikolce Murgovski and Jonas Fredriksson

***Abstract*— This study addresses the computational challenges in optimizing charge planning strategies for electric vehicles (EVs) on long journeys with low ambient temperature. The scale of the problem, its non-linearity and its mixed-integer nature make the problem intractable in real-time applications. This paper introduces a computationally efficient algorithm whose goal is to provide a good trade-off between computation time and accuracy. We achieved this by designing initial guesses for the optimal solution, facilitating the solver's task by starting the optimization process near the desired outcome. We also addressed the mixed-integer nature of the original problem by relaxing its binary variables, allowing it to be solved through gradient-based algorithms. By employing initial guesses and relaxing the boolean variables, the average execution time, compared to running the mixed-integer problem without initial guesses, was reduced by about 91.07%, at the cost of an average increase in energy consumption of only about 0.01%.**

I. INTRODUCTION

In order to meet the increasingly stringent legislation on greenhouse gas emissions, battery electric vehicles (BEVs) are becoming an increasingly popular alternative to internal combustion engine (ICE) vehicles [1]. It is therefore important to facilitate this trend by addressing the issues that make BEVs unappealing. One such issue is their limited range, in combination with long charging times, compared to an ICE vehicle. This, coupled with the fact that charging stations are not as frequent as fossil-fuel refueling stations [2], leads to "range anxiety" [3], that is, the fear of running out of charge before reaching a station.

An intuitive solution to range anxiety is to install larger batteries. However, battery size significantly affects vehicle cost and weight [4]. If increasing the battery size is not feasible, one may try to improve its efficiency. Lithium-ion (Li-ion) batteries operate with sub-optimal efficiency when their temperature is too low (less than $0\,^{\circ}\mathrm{C}$) or too high (above $35\,^{\circ}\mathrm{C}$) [5]. One way to improve the battery's efficiency is by employing battery thermal management (BTM) to ensure that the battery temperature lies within its optimal range. Range anxiety can also be addressed by charge planning, that is, optimally scheduling charging stops so that the vehicle is guaranteed to reach its destination, while also optimizing charging time, energy consumption and waiting times at the stations. In [6], both BTM and charge planning are addressed by formulating a mixed-integer optimization problem through first principles modelling. Besides its mixed-integer nature, additional computational challenges of this optimization problem are its large scale and its non-convexity. Relaxation techniques to efficiently deal with integer variables are explored in [7], where the problem of optimal routing of an electric vehicle is formulated as a stochastic optimization problem, to deal with the randomness of environmental factors. To have an even more computationally feasible solution, [8] introduces an entirely heuristic approach to address a real-world electric vehicle routing problem, which leads to reduced computational cost, compared to optimization-based methods, at the cost of relying on possibly sub-optimal solutions.

Addressing the route and charge planning problems through first principles modelling provides interpretable results. However, the optimization problems formulated through these models tend to be large-scale, non-convex, and mixed-integer, which means it is computationally expensive to solve. Fast solvers, like those employing interior-point methods [9], rely on the calculation of gradients and Hessians, which require having continuous variables. Mixed-integer solvers have to rely on other techniques to efficiently explore the space of the solutions, which, despite the trend of improvements that these solvers are undergoing [10], make them significantly slower compared to their continuous counterparts. The contribution of this paper is to improve the computational viability of first principles modelling methods for electric vehicle routing and charge planning. This is achieved by

- designing an algorithm that generates approximate solutions (initial guesses) to the problem, which are used to warm-start the solver,
- relaxing the discrete variables of the problem so that the solver can treat them like continuous ones.

Our main goal is to show the impact of good initial guesses on the computational viability of optimal methods. Furthermore, generating them requires understanding why certain things are optimal. This has the side-effect of providing useful insights on the problem which may be missed when relying on black-box optimization.

The rest of the paper is structured as follows. Section II introduces the benchmark problem, and the choice of modelling the system in a hybrid space-time formulation is motivated. In section III, the algorithm to generate initial guesses is illustrated in detail. In section IV, the relaxation of the binary variables is addressed. Section V presents the

All authors are with the Department of Electrical Engineering, Chalmers University of Technology, Gothenburg 412 96, Sweden (e-mail: lorenzo.montalto@chalmers.se). This article is within the SEC project CHARGE: Charging and Trip Planning of Electric Vehicles, project number 13048. The authors would also like to thank Viktor Larsson (Volvo Cars), Niklas Legnedahl (Zeekrtech), and Pär-Ola Andersson (E-on) for our fruitful discussions.

results in the form of improvements in computational time compared to the benchmark problem.

II. BENCHMARK PROBLEM

This section introduces the vehicle model, which is based on the one described in [6], and formulates a benchmark optimization problem.

A. Vehicle model

The vehicle is modelled as a nonlinear system

$$\dot{x}(t) = f(x,u) = \begin{bmatrix} f_{T_\mathrm{b}}(x,u) & f_{\mathrm{SoC}}(x,u) \end{bmatrix}^\intercal \tag{1}$$

where, for brevity, nested parentheses in functions have been omitted, i.e., $f(x(t),u(t))$ has been written as $f(x,u)$. The states and control inputs are

$$x(t) = \begin{bmatrix} T_\mathrm{b}(t) & \mathrm{SoC}(t) \end{bmatrix}^\intercal \tag{2}$$

$$u(t) = \begin{bmatrix} P^\mathrm{b}_\mathrm{hvch}(t) & P_\mathrm{grid}(t) & P_\mathrm{hp}(t) & P_\mathrm{hvac}(t) \end{bmatrix}^\intercal \tag{3}$$

where T_b and SoC are battery temperature and state of charge, respectively, $P^\mathrm{b}_\mathrm{hvch}$ is portion of the High Voltage Coolant Heater (HVCH) that heats the battery, and P_grid is charging power taken from the grid, and P_hp and P_hvac are powers of the Heat Pump (HP) and the Heating, Ventilation, and Air Conditioning (HVAC) unit, respectively.

The SoC dynamics are described as

$$f_\mathrm{SoC}(x,u) = -\frac{I_\mathrm{b}(x,u)}{C_\mathrm{b}} = -\frac{P_\mathrm{b}(x,u)}{U_\mathrm{oc}(\mathrm{SoC})C_\mathrm{b}} \tag{4}$$

where C_b, I_b, P_b and U_oc are the battery capacity, current, internal chemical power, and open circuit voltage, respectively. By modeling battery losses as quadratic in current, the battery current can be derived as

$$I_\mathrm{b}(x,u) = \frac{U_\mathrm{oc}(\mathrm{SoC}) - \sqrt{U^2_\mathrm{oc}(\mathrm{SoC}) - 4R_\mathrm{b}(T_\mathrm{b})P_\mathrm{be}(u)}}{2R_\mathrm{b}(T_\mathrm{b})}$$

where the electrical battery power P_be follows from the electric power balance

$$\begin{aligned} P_\mathrm{be}(u) &= P_\mathrm{b}(x,u) - R_\mathrm{b}(\cdot)I^2_\mathrm{b}(\cdot) = P^\mathrm{b}_\mathrm{hvch}(t) + P_\mathrm{hp}(t) \\ &+ P^\mathrm{cab}_\mathrm{hvch}(\cdot) - P_\mathrm{grid}(t) + P_\mathrm{hvac}(t) + P_\mathrm{ed}(t) + P_\mathrm{aux}(t) \end{aligned} \tag{5}$$

where

$$P^\mathrm{cab}_\mathrm{hvch}(\cdot) = \frac{P_\mathrm{c}(T_\mathrm{amb}) - \eta_\mathrm{hp}(\mathrm{cop}_\mathrm{hp1}T_\mathrm{b}(t) + \mathrm{cop}_\mathrm{hp0})P_\mathrm{hp}(t)}{\eta_\mathrm{Qhvch}}$$

is the portion of HVCH power to heat up the cabin compartment, P_ed is the power of the electric drive unit that propels the vehicle, P_aux is the power consumed by other auxiliary devices, P_c is the power demand for cabin heating, computed as a function of ambient temperature T_amb, and η_Qhvch is the electrical-to-heat efficiency of the HVCH for cabin heating. The battery resistance and open circuit voltage are modeled as polynomial functions

$$R_\mathrm{b}(T_\mathrm{b}) = \begin{bmatrix} T_\mathrm{b}(t)^2 & T_\mathrm{b}(t) & 1 \end{bmatrix}^\intercal r_\mathrm{b} \tag{6}$$

$$U_\mathrm{oc}(\mathrm{SoC}) = \begin{bmatrix} \mathrm{SoC}^2(t) & \mathrm{SoC}(t) & 1 \end{bmatrix}^\intercal u_\mathrm{oc} \tag{7}$$

where $r_\mathrm{b} \in \mathbb{R}^{3\times 1}$ and $u_\mathrm{oc} \in \mathbb{R}^{3\times 1}$ are coefficients determined by fitting existing data.

The temperature dynamics are described as

$$\begin{aligned} f_{T_\mathrm{b}}(x,u) = \frac{1}{c_\mathrm{b}m_\mathrm{b}}\Big(& R_\mathrm{b}(T_\mathrm{b})I^2_\mathrm{b}(x,u) + \eta_\mathrm{hvch}P^\mathrm{b}_\mathrm{hvch}(t) \\ & + \eta_\mathrm{Qed}(1-\eta_\mathrm{ed})|P_\mathrm{ed}(t)| - \mathrm{cop}_\mathrm{hvac}P_\mathrm{hvac}(t) \\ & - (\mathrm{cop}_\mathrm{hp1}T_\mathrm{b}(t) + \mathrm{cop}_\mathrm{hp0} - 1)P_\mathrm{hp}(t) \\ & - (\gamma_0 + \gamma_1 v^{\gamma_2}(t))(T_\mathrm{b}(t) - T_\mathrm{amb})\Big) \end{aligned} \tag{8}$$

where c_b is the heat capacity of the battery cells and m_b is the mass of the battery pack. The terms in the outer parentheses represent, respectively: the Joule heat due to battery resistive losses; the heat of the HVCH, where η_hvch is HVCH efficiency; the heat of the electric drive, where η_ed and η_Qed are electrical to mechanical and electrical to heat efficiency of the electric drive; the portion of the HVAC heat that goes to the battery, where $\mathrm{cop}_\mathrm{hvac}$ is its coefficient of performance; the heat of the HP, where $\mathrm{cop}_\mathrm{hp0}$ and $\mathrm{cop}_\mathrm{hp1}$ are its coefficients of performance; and the convective heat exchange between the battery pack and the ambient, v is the vehicle speed, and γ_0, γ_1 and γ_2 are coefficients related to parasitic heat transfer.

The HVCH power for battery heating is constrained as

$$0 \le P^\mathrm{b}_\mathrm{hvch}(t) \le P^\mathrm{max}_\mathrm{hvch} - P^\mathrm{cab}_\mathrm{hvch}(t) \tag{9}$$

where $P^\mathrm{max}_\mathrm{hvch}$ is the maximum HVCH power that could be used if the cabin compartment was not being heated.

The vehicle speed $v(t)$ and the powers $P_\mathrm{ed}(t)$ and $P_\mathrm{aux}(t)$ are considered as deterministic inputs. These signals are generally estimated with a predictor, the functionality of which is outside this paper's scope. Moreover, since this paper investigates the development of computationally efficient algorithms, for fairness of comparison, the same input signals, measured on a previously driven route, are used both in the benchmark and the proposed method.

B. Charging and driving modes

The input signals $v(t)$, $P_\mathrm{ed}(t)$ and $P_\mathrm{aux}(t)$ include only time instants when the vehicle is driven on the main route, without including the detour segments to and from chargers. In fact, for all other driving instants it strictly holds $v(t) > 0$.

Let $\Delta x_{\mathrm{det}i}$ represent the change of the state variables due to a detour to or from charger $i = 1,\dots,N_\mathrm{c}$, where N_c is the number of available chargers near the main route. Let $\mathcal{S}_\mathrm{c} = \{s_{\mathrm{c}1},\dots,s_{\mathrm{c}N_\mathrm{c}}\}$ represent the set of locations on the main route where the detour starts and ends. We attach subscripts c and d to distinguish signals between charging and driving modes. Then, to impose continuity between driving and charging modes, we impose the constraints

$$x_{\mathrm{c}i}(t_{0i}) = x_\mathrm{d}(s_{ci}) + c_i\Delta x_{\mathrm{det}i}, \quad i = 1,\dots,N_\mathrm{c} \tag{10a}$$

$$x_\mathrm{d}(s^+_{ci}) = x_{\mathrm{c}i}(t_{\mathrm{f}i}) + c_i\Delta x_{\mathrm{det}i}, \quad i = 1,\dots,N_\mathrm{c} \tag{10b}$$

where $c_i \in \{0,1\}$ is a binary decision variable that is 1 if the vehicle visits charger i. The first constraint indicates that the states $x_{ci}(t_{0i})$, when charging at station i starts, equal the states $x_\mathrm{d}(s_{ci})$, when the vehicle reached location s_{ci} on the main route, plus the change in state value due to the detour. The second constraint indicates that the states $x_\mathrm{d}(s^+_{ci})$

at position s_{ci}^+, just after charger i, equal the states $x_{ci}(t_{\mathrm{f}i})$, when the vehicle finished charging, plus the change in value due to the detour for coming back to the main route. Notice that, for simplicity, the same detour value $\Delta x_{\mathrm{det}i}$ is used both to and from the chargers. However, the studied algorithms are general and can be applied even when $\Delta x_{\mathrm{det}i}$ differ in the different detour directions, or when location s_{ci}^+ is further away from s_{ci}.

The vehicle operation also differs in driving and charging modes. This is described by a set of conditions,

$$
\begin{aligned}
&P_{\mathrm{grid}}(t) = 0, && t \notin [t_{0i}, t_{\mathrm{f}i}] && \text{(11a)}\\
&P_{\mathrm{b}}(x_{\mathrm{d}}, u_{\mathrm{d}}) \in [P_{\mathrm{bd}}^{\min}(x_{\mathrm{d}}), P_{\mathrm{bd}}^{\max}(x_{\mathrm{d}})], && t \notin [t_{0i}, t_{\mathrm{f}i}] && \text{(11b)}\\
&P_{\mathrm{grid}}(t) \in [0, c_i P_{\mathrm{grid}i}^{\max}], && t \in [t_{0i}, t_{\mathrm{f}i}] && \text{(11c)}\\
&P_{\mathrm{ed}}(t) = P_{\mathrm{aux}}(t) = v(t) = 0, && t \in [t_{0i}, t_{\mathrm{f}i}] && \text{(11d)}\\
&P_{\mathrm{b}}(x_{ci}, u_{ci}) \in [c_i P_{\mathrm{bc}}^{\min}(x_{ci}), 0], && t \in [t_{0i}, t_{\mathrm{f}i}] && \text{(11e)}
\end{aligned}
$$

imposed for all $i = 1, \ldots, N_{\mathrm{c}}$. Here, $P_{\mathrm{grid}i}^{\max}$ is the maximum charging power station i may provide, $P_{\mathrm{bc}}^{\min}$ is the battery charging power limit, and $P_{\mathrm{bd}}^{\min}$ and $P_{\mathrm{bd}}^{\max}$ are the battery discharging power limits. These power limits follow the same behavior as the ones in [6].

C. Spatial coordinates in driving mode

Following [6], we use driven distance s as the independent variable in driving mode. This does not bring clear benefits in this study, since the vehicle speed is assumed to be known. However, [6] discusses its benefits when speed is uncertain or part of the state vector.

As mentioned earlier, during driving it is assumed that $v(t) > 0$. Then, $x_{\mathrm{d}}(t) = x_{\mathrm{d}}(s(t)) = x_{\mathrm{d}}(s)$. Each state value in time can uniquely be described as a function of the position s, and it is possible to sample the signals directly in s. The state derivatives during driving mode now change to

$$
\frac{\mathrm{d}x_{\mathrm{d}}(s)}{\mathrm{d}s} = \frac{1}{v(s)} f(x_{\mathrm{d}}, u_{\mathrm{d}}) = f_{\mathrm{d}}(x_{\mathrm{d}}, u_{\mathrm{d}}). \tag{12}
$$

Sampling in time is preserved only in charging mode. Hence, for simplicity, the start of the charging time can be assumed zero, i.e., $t_{0i} = 0$, for all $i = 1, \ldots, N_{\mathrm{c}}$.

D. Normalized time in charging mode

The charging time $t_{\mathrm{f}i}$ at station i is not known in advance, i.e., it is a decision variable. To formulate the problem as a standard optimal control program, it is beneficial to use normalized time $\tau_i \in [0, 1]$ as the independent variable in charging mode. The actual time can then be expressed as $t_i = t_{\mathrm{f}i}\tau_i$, while the state derivatives during charging mode now change to

$$
\frac{\mathrm{d}x_{\mathrm{c}i}(\tau_i)}{\mathrm{d}\tau_i} = t_{\mathrm{f}i} f(x_{ci}, u_{ci}). \tag{13}
$$

E. Problem statement

The problem is formulated to minimize a weighted cost between charging time and energy taken from the grid,

$$
J(\cdot) = \sum_{i=1}^{N_{\mathrm{c}}} \left(w_{\mathrm{t}} t_{\mathrm{f}i} + w_{\mathrm{s}} c_i + w_{\mathrm{e}} t_{\mathrm{f}i} \int_0^1 P_{\mathrm{grid}}(\tau_i) \mathrm{d}\tau_i \right) \tag{14}
$$

where w_t and w_{e} translate time and energy to monetary costs. The weight w_{s} is used to assign a cost due to detour time when stopping at chargers.

Considering both driving and charging modes, the states and control sequences can be collected as

$$
\boldsymbol{x} = \{x_{\mathrm{d}}(s), x_{ci}(\tau_i)\}, \quad \boldsymbol{u} = \{u_{\mathrm{d}}(s), u_{ci}(\tau_i)\}, \tag{15}
$$

for all $s \in [0, s_{\mathrm{f}}]$, for all $i = 1, \ldots, N_{\mathrm{c}}$, and all $\tau_i \in [0, 1]$, where s_{f} is the final position. Let the vectors of charging times and binary charging decisions be defined as

$$
\boldsymbol{t}_{\mathrm{f}} = \begin{bmatrix} t_{\mathrm{f}1} & \ldots & t_{\mathrm{f}N_{\mathrm{c}}} \end{bmatrix}^{\intercal}, \quad \boldsymbol{c} = \begin{bmatrix} c_1 & \ldots & c_{N_{\mathrm{c}}} \end{bmatrix}^{\intercal}. \tag{16}
$$

Then, the optimal control problem can be stated as

$$
\begin{aligned}
&\min_{\boldsymbol{x}, \boldsymbol{u}, \boldsymbol{t}_{\mathrm{f}}, \boldsymbol{c}} J(\boldsymbol{x}, \boldsymbol{u}, \boldsymbol{t}_{\mathrm{f}}, \boldsymbol{c}) && && \text{(17a)}\\
&\quad \text{s.t.: (9), (11), } x_{\mathrm{d}}(0) = x_{\mathrm{d}0},\ x_{\mathrm{d}}(s_{\mathrm{f}}) \in \mathbb{X}_{\mathrm{f}} && && \text{(17b)}\\
&\qquad \frac{\mathrm{d}x_{\mathrm{d}}(s)}{\mathrm{d}s} = \frac{1}{v(s)} f(x_{\mathrm{d}}, u_{\mathrm{d}}), \quad s \in [0, s_{\mathrm{f}}] && && \text{(17c)}\\
&\qquad \frac{\mathrm{d}x_{ci}(\tau_i)}{\mathrm{d}\tau_i} = t_{\mathrm{f}i} f(x_{ci}, u_{ci}), \tau_i \in [0, 1], s = s_{ci} && && \text{(17d)}\\
&\qquad x_{ci}(0) = x_{\mathrm{d}}(s_{ci}) + c_i \Delta x_{\mathrm{det}i} && && \text{(17e)}\\
&\qquad x_{\mathrm{d}}(s_{ci}^+) = x_{ci}(1) + c_i \Delta x_{\mathrm{det}i} && && \text{(17f)}\\
&\qquad \boldsymbol{x} \in \mathbb{X}, \boldsymbol{u} \in \mathbb{U}, \boldsymbol{t}_{\mathrm{f}} \in \mathbb{T}, \boldsymbol{c} \in \{0, 1\}^{N_{\mathrm{c}}} && && \text{(17g)}
\end{aligned}
$$

where constraints (17d)-(17f) are imposed for all $i = 1, \ldots, N_{\mathrm{c}}$, constraints (11a)-(11b) are imposed for all $s \in [0, s_{\mathrm{f}}]$, and (11c)-(11e) are imposed for all $\tau_i \in [0, 1]$. The sets $\mathbb{X}_{\mathrm{f}}$, $\mathbb{X}$, $\mathbb{U}$, $\mathbb{T}$ are constructed by imposing typical box constraints on the optimization variables.

Problem (17) is discretized using fourth order explicit Runge Kutta method. The resulting problem is a computationally heavy mixed-integer, nonlinear optimization program. In the following, we provide two methods to reduce computation time, 1) by providing a good initial guess for the optimization variables, and 2) relaxing the binary variables.

III. Initial guesses

What follows is a description of how the algorithm selects the charging stations and the control inputs to construct the initial guesses to warm-start the solver. The initial guesses for the decision variables in (17) are indicated with the same symbols but with a tilde on top.

The initial guess for the control inputs is based on properties of the benchmark problem's optimal solution. In particular, it has been observed that the HVAC is never used, i.e., we consider $\tilde{P}_{\mathrm{hvacd}}(s) = 0$, $\forall s$ and $\tilde{P}_{\mathrm{hvacc}}(t_i) = 0$, $\forall t_i$.

A. Charging stations selection

This section proposes a strategy to provide initial guesses $\tilde{c}_j$ for selected charging stations $j \in \mathbb{J} \subseteq \{1, \dots, N_\mathrm{c}\}$, where the states are simulated forward according to (12) and without using HVCH and HP. This simulation represents a prediction of how far the vehicle can go without charging and without actively controlling the battery temperature.

The simulation starts with an initial guess for the SoC,

$$\widetilde{\mathrm{SoC}}_\mathrm{d}(s) = \begin{cases} \mathrm{SoC}_\mathrm{d}(0), & s = 0 \\ \widetilde{\mathrm{SoC}}_\mathrm{d}(s_{cj}^+), & s = s_{\mathrm{c}j} \end{cases} \tag{18}$$

which is either that at the start of the trip or after charging is performed at station j, i.e,

$$\widetilde{\mathrm{SoC}}_\mathrm{d}(s_{\mathrm{c}j}^+) = \widetilde{\mathrm{SoC}}_{\mathrm{c}j}(1) + \Delta\mathrm{SoC}_{\mathrm{det}j}$$

with $\Delta\mathrm{SoC}_{\mathrm{det}j} \leq 0$. Then, simulation is carried over s until one of two possible conditions is reached. Either the destination s_f is reached, which means no further chargers are selected, or $\widetilde{\mathrm{SoC}}_\mathrm{d}(s)$ drops below a certain threshold $\mathrm{SoC}_\mathrm{low} > 0$, chosen to provide a robust margin due to the possibly sub-optimal choices of the control inputs. When the latter happens, backtracking is performed to find the nearest previous charging station, which is added to the set $\mathbb{J}$. This simulation also provides the initial guess

$$\widetilde{\mathrm{SoC}}_{\mathrm{c}j}(0) = \widetilde{\mathrm{SoC}}_\mathrm{d}(s_{\mathrm{c}j}) + \Delta\mathrm{SoC}_{\mathrm{det}j}$$

at which charging starts at station j.

The guess of the value at which charging at station j stops is found by first simulating forward over $s > s_{\mathrm{c}j}$, similarly as above. Let $\mathrm{SoC}_\mathrm{sim}(s)$ be the simulated SoC until either the destination is reached, or the next charging station j^+ is selected. Then,

$$\widetilde{\mathrm{SoC}}_{\mathrm{c}j}(1) = \begin{cases} \mathrm{SoC}_\mathrm{high}, & s_{\mathrm{c}j^+} < s_\mathrm{f} \\ \mathrm{SoC}_\mathrm{high} + \mathrm{SoC}_\mathrm{low} - \mathrm{SoC}_\mathrm{sim}(s_\mathrm{f}), & s = s_\mathrm{f} \end{cases}$$

where $\mathrm{SoC}_\mathrm{high} < 1$ is an upper bound chosen to provide a reasonable trade-off between having sufficient energy to drive the next segment and not waiting too long to charge the last few percents in the battery [6]. In other words, if we detect that the destination can be reached in the next segment, then there is no need to charge the battery more than necessary to reach the destination.

B. Control inputs in driving mode

The previous subsection provided a strategy to select chargers and the guess for initial and final SoC during charging. Here, we improve the guess for SoC during driving.

The journey is divided into driving segments, delimited by two consecutive charging stations. In these segments, HVCH and HP ensure the vehicle reaches the next station with the desired battery temperature $T_\mathrm{b,des}$ to optimize charging [5]. This temperature optimization process is called preconditioning. What follows is a description of how HVCH and HP power profiles are decided for a generic driving segment $[s_{\mathrm{c}j-1}, s_{\mathrm{c}j}]$. Since the first and the last driving segments are not delimited by two charging stations, they are defined differently. Namely, the first driving segment is $[0, s_{\mathrm{c}1}]$, while the last is $[s_{\mathrm{c}N_\mathrm{c}}, s_\mathrm{f}]$.

A useful assumption on the power profile of the HVCH, made in [11], is that it is turned on at a constant power when preconditioning starts and then turned off when the vehicle reaches the station (an assumption based on empirical observations of its optimal power profile). Such power profile can then be defined as

$$\tilde{P}^\mathrm{b}_\mathrm{hvchd}(s) = \begin{cases} P_{\mathrm{hvchg}j}, & \text{for } s \in [s^*_{\mathrm{on}j}, s_{\mathrm{c}j}] \\ 0, & \text{otherwise} \end{cases}, \quad j \in \mathbb{J} \tag{19}$$

where $P_{\mathrm{hvchg}j}$ is the constant HVCH power used to reach the desired battery temperature and $s^*_{\mathrm{on}j} < s_{\mathrm{c}j}$ is the optimal location to turn on the HVCH. Another useful assumption, also based on empirical observations of the optimal power profile of the HVCH, is that it is optimal to use HVCH at its maximum power for the shortest amount of time necessary to reach the desired battery temperature. Therefore, only $s^*_{\mathrm{on}j}$ has to be computed. The preconditioning scheme follows a strategy similar to [11], where one backward and multiple forward simulations are combined to obtain the control inputs trajectories during preconditioning.

The backward simulation starts from the desired temperature $T_\mathrm{b,des}$ and the SoC level when reaching the charging station $\mathrm{SoC}_{\mathrm{chg}j}$. Obtaining a closed form of the inverted dynamics is challenging due to the nonlinearities in f_d. Therefore, we settle for an approximate solution, where the dynamics of the linearized system are inverted instead. First, (12) is discretized with Euler's method as

$$x_\mathrm{d}^+ = x_\mathrm{d} + f_\mathrm{d}(x_\mathrm{d}, u_\mathrm{d}) \cdot \Delta s \tag{20}$$

where Δs is the sampling interval in space domain. Then, f_d is linearized around x_d^+

$$f_\mathrm{d}(x_\mathrm{d}, u_\mathrm{d}) \approx f_\mathrm{d}(x_\mathrm{d}^+, u_\mathrm{d}) + \nabla_{x_\mathrm{d}} f_\mathrm{d}(x_\mathrm{d}^+, u_\mathrm{d})(x_\mathrm{d} - x_\mathrm{d}^+) \tag{21}$$

where $\nabla_{x_\mathrm{d}} f_\mathrm{d}$ is the Jacobian of f_d with respect to the state vector x_d. Combining (20) and (21), x_d can be expressed as a function of x_d^+, and thus the backward dynamics are obtained as

$$x_\mathrm{d} \approx x_\mathrm{d}^+ - \Delta s \left(I + \nabla_{x_\mathrm{d}} f_\mathrm{d}(x_\mathrm{d}^+, u_\mathrm{d}) \Delta s\right)^{-1} f(x_\mathrm{d}^+, u_\mathrm{d}). \tag{22}$$

During the backward simulation, HVCH is used at its upper limit, as per (9), and the HP is not used. The states obtained through backward simulation are denoted as $\tilde{x}_{\mathrm{d,bw}}$.

For the forward simulations, $P_\mathrm{hpd}(s)$ is gridded into N_fw values and a simulation is performed for each one of them. The states obtained through forward simulation with the kth value of $P_\mathrm{hpd}(s)$, with $k \in \{1, \dots, N_\mathrm{fw}\}$, are denoted as $\tilde{x}^k_{\mathrm{d,fw}}$. Each forward simulation is performed until the battery temperature intersects the backwards one, that is until $\tilde{T}^k_{\mathrm{bd,fw}}(s) = \tilde{T}_{\mathrm{bd,bw}}(s)$. The location s for which this happens is denoted as $s_{\mathrm{on}j}$. During the forward simulations HVCH is not used.

Finally, the forward simulations and the backward one are combined to obtain N_{fw} possible preconditioning trajectories

$$\tilde{x}^k_{\mathrm{d,prec}} = \begin{cases} \tilde{x}^k_{\mathrm{d,fw}}(s), \text{ if } s \in [s_{cj-1}, s^k_{\mathrm{on}j}) \\ \tilde{x}_{\mathrm{d,bw}}(s), \text{ if } s \in [s_{\mathrm{on}j}, s_{cj}] \end{cases} \tag{23}$$

where $s_{cj-1} = 0$, if $j = 1$. The total cost of each of these trajectories is the total energy used by the battery during preconditioning. The optimal location where to turn on HVCH is then obtained as

$$s^*_{\mathrm{on}j} = \arg\min_{s^k_{\mathrm{on}j}} \int_{s_{cj-1}}^{s_{cj}} \frac{\tilde{P}^k_{\mathrm{bd}}(s)}{v(s)} \mathrm{d}s. \tag{24}$$

During the last driving segment, a similar procedure is applied but without HVCH, since no more preconditioning will be needed.

In every driving segment, $\tilde{P}_{\mathrm{bd}}$ is decided to ensure energy balance according to (5) and it is constrained according to (11b).

C. Control inputs in charging mode

Charging is performed with maximum available power

$$\tilde{P}_{\mathrm{bc}}(t) = P^{\min}_{\mathrm{bc}}(x_{\mathrm{c}i}) \tag{25}$$

until the desired SoC level is reached. As the battery temperature may continue increasing due to Joule losses, we must ensure that it does not rise above $T_{\mathrm{b,max}}$. This can be achieved by employing the HP whenever $T_{\mathrm{b,max}}$ is reached. To obtain the power profile of the HP needed to keep the battery temperature constant, (8) is set to 0 and solved for $P_{\mathrm{hpc}}(t)$, knowing that, while charging, $P_{\mathrm{ed}}(t) = v(t) = P_{\mathrm{hvacc}}(t) = P^{\mathrm{b}}_{\mathrm{hvchc}}(t) = 0$. Taking into account its power limits, the power profile of the HP to saturate the battery temperature during charging is then obtained as

$$\tilde{P}_{\mathrm{hp,sat}}(t) = \max\{\min\{\frac{R_{\mathrm{bc}}(t)I^2_{\mathrm{bc}}(t) - \gamma_0(T_{\mathrm{b,max}} - T_{\mathrm{amb}})}{\mathrm{cop}_{\mathrm{hp1}}T_{\mathrm{bc}} + \mathrm{cop}_{\mathrm{hp0}} - 1}, P^{\max}_{\mathrm{hp}}\}, P^{\min}_{\mathrm{hp}}\}. \tag{26}$$

From this, the entire power profile of the HP during charging can be defined as

$$\tilde{P}_{\mathrm{hpc}}(t) = \begin{cases} \tilde{P}_{\mathrm{hp,sat}}(t), & \text{if } \tilde{T}_{\mathrm{bc}}(t) \geq T_{\mathrm{b,max}} \\ 0, & \text{otherwise.} \end{cases} \tag{27}$$

IV. Relaxation of binary variables

The initial guesses from Section III may shorten computation time of solving problem (17). However, charging location guesses may be infeasible. The goal is to allow the optimizer flexibility to select different chargers without solving a mixed-integer problem. To do this, the binary variables introduced in (10) have been relaxed into continuous ones, which are indicated as c^r_i. This relaxation has been achieved by introducing a set of constraints into the benchmark problem

$$0 \leq c^r_i \leq 1, \qquad i = 1, \ldots, N_{\mathrm{c}} \tag{28a}$$
$$c^r_i \cdot (1 - c^r_i) \leq \epsilon_i, \qquad i = 1, \ldots, N_{\mathrm{c}} \tag{28b}$$
$$\epsilon_i \geq 0, \qquad i = 1, \ldots, N_{\mathrm{c}} \tag{28c}$$

where $\epsilon^i \in \mathbb{R}$ is a slack variable for charging station i and is used to achieve the relaxation. The way these constraints work is that, even though (28a) allows the values of c^r_i to be within 0 and 1, (28b) and (28c) force it to be very close to either 0 or 1. For this to work, ϵ_i needs to be as close as possible to 0, which is done by introducing an additional term in the cost function of the benchmark problem (14)

$$J_{\mathrm{new}} = J + \rho \sum_{i=1}^{N_{\mathrm{c}}} \epsilon_i \tag{29}$$

where ρ is a penalty term to tune the weight of this additional term into the original cost function.

Algorithm 1: Generation of initial guesses

Data: s_0, s_f, charging stations, vehicle's model
Result: $\tilde{x}_d$, $\tilde{u}_d$, $\tilde{x}_c$, $\tilde{u}_c$, $\tilde{c}$

```
for s ← s_0 to s_f do
    if Not in last driving cycle then
        Compute P̃_bd(s) as in (5) and (11b) to ensure energy balance;
        Forward simulation of x̃_d(s) as in (12), with P^b_hvchd(s) = P_hpd(s) = 0;
        if SoC_d < SoC_lim then
            Find nearest previous charging station and compute desired SoC level as in III-A;
            if A charging station was found then
                if T̃_bd is too low for charging then
                    Do preconditioning as in III-B;
                Compute charging control inputs as in III-C;
                Forward simulation of x̃_c(t) as in (1);
    else
        Compute driving control inputs for last driving cycle as in III-B but without HVCH;
        Forward simulation of x̃_d(s) as in (12);
```

V. Results

We compare the average execution time over 12 runs of 1) the original benchmark problem with binary variables and no warm-start, 2) our improved optimization with relaxed binary variables and warm-start and 3) the initial guesses alone. Each run has a unique ambient temperature and chargers configuration. The tests ran on a machine with 32GB RAM, 1.8GHz processor and 64-bit Windows 10. The benchmark problem was solved on MATLAB with CasADi, using IPOPT as a solver. Table II shows the simulations parameters.

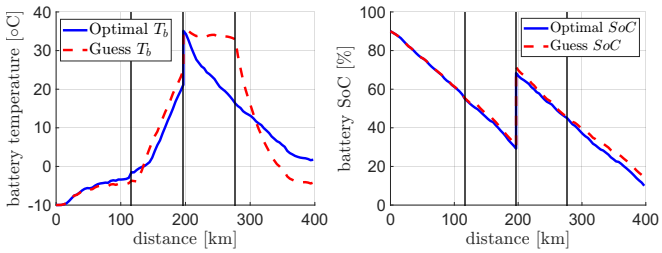

(a) Driving mode. (b) Driving mode.

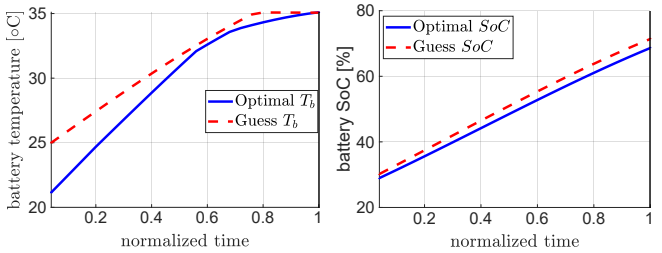

(c) Charging mode. (d) Charging mode.

Fig. 1: Comparison between optimal and guessed state trajectories.

Note that P_{aux} has been considered constant throughout the simulations. Fig. 2 shows speed and propulsion power profiles for all tests. Table I shows the main results for computational time and driving energy.

TABLE I: Difference in computational time and drive energy

	Benchmark	With impr.	Init. guesses
Avg time [s]	77.95	6.69	0.09
Avg drive energy [kWh]	94.01	94.11	94.19

Relaxing the binary variables and warm-starting the solver reduces the average execution time by 91.07%, while the average driving energy consumption increases by 0.01%. For the initial guesses alone, the average driving energy is 0.19% more than case 1 and 0.09% more than case 2. Despite the initial guesses leading to a near-optimal driving energy consumption, relying on optimization guarantees feasibility and optimality. Furthermore, the tests were all done on the same drive cycle, so close resemblance in driving energy may not apply to any cycle. Finally, the similarity is only in driving energy. Charging energy comparison is not possible, as we do not guess charging time.

Fig. 1 shows an example run comparing guess trajectories (dashed red) and optimal ones (blue) for the state variables, both for driving and for charging modes. Note that time is normalized during charging, since charging time is a decision variable. The simulation has been performed at an ambient temperature of $T_{\text{amb}} = -10\,^{\circ}\text{C}$, so that preconditioning of the battery would be necessary. The three vertical black lines represent the charging stations along the way. The SoC trajectory shows that both the initial guess and the optimal solution chose the second charging station to recharge the battery.

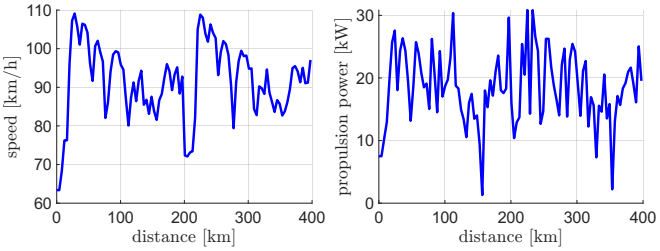

(a) Speed profile (b) Propulsion power profile

Fig. 2: Speed and propulsion power profiles.

TABLE II: Parameters used during the simulations

$\text{cop}_{\text{hp0}} = 1.92$, $\text{cop}_{\text{hp1}} = 0.07\,\text{K}^{-1}$, $\text{cop}_{\text{hvac}} = 3$
$\gamma_1 = 8.54\,\text{W h km}^{-1}\,\text{K}^{-1}$, $\gamma_2 = 0.45$, $c_{\text{b}} = 1015\,\text{J kg}^{-1}\,\text{K}^{-1}$
$m_{\text{b}} = 371.79\,\text{kg}$, $C_{\text{b}} = 7.02 \times 10^5\,\text{A s}$, $\eta_{\text{hvch}} = 0.87$, $\eta_{\text{hp}} = 0.95$
$\eta_{\text{Qed}} = 0.8$, $\eta_{\text{ed}} = 0.9$, $\eta_{\text{Qhvch}} = 0.95$, $N_{\text{fw}} = 10$
$\Delta s = 4.02\,\text{km}$, $r_{\text{b}} = [0, 0.001, -0.32, 32.71]^\intercal\ \Omega K^{-1}$
$u_{\text{oc}} = [85.3, -5.51, 382.85]^\intercal$ V, $\gamma_0 = 9.2\,\text{W K}^{-1}$
$T_{\text{b,des}} = 298.15\,\text{K}$, $T_{\text{b,max}} = 308.15\,\text{K}$, $w_{\text{t}} = 0.07\,\text{SEK h}^{-1}$
$w_{\text{s}} = 20.83\,\text{SEK stop}^{-1}$, $w_{\text{e}} = 2.42 \times 10^{-8}\,\text{SEK W}^{-1}\,\text{h}^{-1}$
$\rho = 10\,\text{SEK stop}^{-1}$, $P_{\text{c}} = 2.6\,\text{kW}$, $P_{\text{hvch}}^{\max} = 7\,\text{kW}$
$P_{\text{aux}} = 0.5\,\text{kW}$, $\text{SoC}_{\text{low}} = 10\%$, $\text{SoC}_{\text{high}} = 100\%$

References

[1] J. Jaguemont, L. Boulon, P. Venet, Y. Dubé, and A. Sari, "Lithium-ion battery aging experiments at subzero temperatures and model development for capacity fade estimation," *IEEE Transactions on Vehicular Technology*, vol. 65, no. 6, pp. 4328–4343, 2016.

[2] M. Ahmadi, N. Mithulananthan, and R. Sharma, "A review on topologies for fast charging stations for electric vehicles," in *2016 IEEE International Conference on Power System Technology (POWERCON)*, pp. 1–6, 2016.

[3] N. Rauh, T. Franke, and J. F. Krems, "Understanding the impact of electric vehicle driving experience on range anxiety," *Human Factors*, vol. 57, no. 1, pp. 177–187, 2015. PMID: 25790577.

[4] M. Redelbach, E. D. Özdemir, and H. E. Friedrich, "Optimizing battery sizes of plug-in hybrid and extended range electric vehicles for different user types," *Energy Policy*, vol. 73, pp. 158–168, 2014.

[5] C. Zhu, F. Lu, H. Zhang, and C. C. Mi, "Robust predictive battery thermal management strategy for connected and automated hybrid electric vehicles based on thermoelectric parameter uncertainty," *IEEE Journal of Emerging and Selected Topics in Power Electronics*, vol. 6, no. 4, pp. 1796–1805, 2018.

[6] A. Hamednia, N. Murgovski, J. Fredriksson, J. Forsman, M. Pourabdollah, and V. Larsson, "Optimal thermal management, charging, and eco-driving of battery electric vehicles," *IEEE Transactions on Vehicular Technology*, vol. 72, no. 6, pp. 7265–7278, 2023.

[7] Z. Yi and P. H. Bauer, "Optimal stochastic eco-routing solutions for electric vehicles," *IEEE Transactions on Intelligent Transportation Systems*, vol. 19, no. 12, pp. 3807–3817, 2018.

[8] M. Zhao and Y. Lu, "A heuristic approach for a real-world electric vehicle routing problem," *Algorithms*, vol. 12, no. 2, 2019.

[9] F. A. Potra and S. J. Wright, "Interior-point methods," *Journal of Computational and Applied Mathematics*, vol. 124, no. 1, pp. 281–302, 2000. Numerical Analysis 2000. Vol. IV: Optimization and Nonlinear Equations.

[10] T. Achterberg and R. Wunderling, *Mixed Integer Programming: Analyzing 12 Years of Progress*, pp. 449–481. Berlin, Heidelberg: Springer Berlin Heidelberg, 2013.

[11] A. Hamednia, J. Forsman, N. M. V. Larsson, and J. Fredriksson, "Computationally efficient approach for preheating of battery electric vehicles before fast charging in cold climates," *IFAC-PapersOnLine*, vol. 56, no. 2, pp. 6630–6635, 2023. 22nd IFAC World Congress.